Atomic layer deposited α−MoO_3 thin films as a promising solid-state hydrogen storage material

David Maria Tobaldi,[a,*] Vittorianna Tasco,[a] Gianluca Balestra,[a] Daniela Lorenzo,[a] Maria Grazia Manera,[b] Adriana Passaseo,[a] Marco Esposito,[a] and Massimo Cuscunà[a,*]

[a]*CNR Nanotec, Institute of Nanotechnology, University Campus Ecotekne, Via per Monteroni, 73100 Lecce, Italy*

[b]*CNR IMM, Institute for Microelectronic and Microsystems, University Campus Ecotekne, Via per Monteroni, 73100 Lecce, Italy*

Abstract

Hydrogen has the potential to become a crucial energy storage vector, allowing to maximise the advantages of renewable and sustainable energy sources. Hydrogen is usually stored as compressed hydrogen gas, or liquid hydrogen. However, the former requires high pressure, the latter cryogenic temperatures, being a huge limit to the widespread adoption of these storage methods. Thus, new materials for solid-state hydrogen storage shall be developed. Here we show that a α−MoO_3 thin film, grown *via* atomic layer deposition, is a promising material for reversibly storing hydrogen. We found that hydrogen plasma is a convenient way to hydrogenise − at room temperature and relatively low pressures (500 or 1000 mTorr) − layered monocrystalline α−MoO_3 thin films. Hydrogen has been shown to locate itself in the van der Waals gap along the [010] oriented α−MoO_3 film. The process has been found to be totally reversible in air. Our essay could be a starting point to a transition from conventional (gas and liquid) to more advantageous solid-state hydrogen storage materials.

KEYWORDS: Energy materials; Solid-state hydrogen storage; Reversible hydrogenation; Molybdenum oxide; Atomic layer deposition; Hydrogen plasma

*Corresponding authors.

E-mail addresses: david.tobaldi@nanotec.cnr.it; massimo.cuscuna@nanotec.cnr.it

1. Introduction

Most of the energy exploited by human-kind has been essentially achieved by using fossil-fuels [1]. While this boosted the *Industrial Revolution* leading to a global economic growth, the release of greenhouse gases contributed to the environmental concerns we are experiencing nowadays [2]. A new collective conscience is globally spreading to replace the old carbon-based society with a carbon-neutral one. As a consequence, United Nations' *Net Zero Coalition* aims to reduce greenhouse gas emissions by 45% by 2030, to reach net zero by 2050 [3]. To this aim, the challenge is providing a sustainable supply of clean and green energy, as the new normal shall follow the regime of renewable energy sources [4]. Hydrogen, being a zero-emission fuel, is the ideal candidate to replace fossils-fuels. Being green and clean, storable, and transportable, it is foreseen to play an important role in solving energy and environmental issues [5]. Hydrogen-based energy storage systems are gaining momentum as a cost-effective solution for a large-scale renewable energy storage, transport and export [6]. However, being a fuel itself, it naturally comes together with some degree of safety concerns, as it is conventionally stored at high-pressure as a gas, or as a liquid at cryogenic temperatures [7]. The primary risk is therefore associated with leakage or boil-off losses, as hydrogen is highly prone to spontaneously combust [8].

Considering the energy crisis we are facing, storage is one serious bottle-neck to overtake. Indeed, safer and alternative materials for solid-state hydrogen storage are strongly desired. Materials-based hydrogen solid-state storage devices are a captivating alternative. However, most of those based on chemisorption (*i.e.* hydrides, nitrides, imides) are generally costly, and have irreversible hydrogen absorption/desorption processes. Additionally, some of these materials involve very high temperatures for hydrogen release [9]. Thus, advances in energy storage require materials fabricated at the nanoscale [10]. Materials having a layered structure are drawing attention as candidates to energy storage devices, with molybdenum oxide (MoO_3) being one of the most appealing [11], as also recently proven by Goncalves *et al*. by means of computational investigation [12].

MoO_3 crystallises in several polymorphs, the orthorhombic molybdite (α−MoO_3) being the thermodynamically stable and natural occurring of them [13]. Crystal structure of α−MoO_3 is described in the space group *Pbnm* (with 4 formula units per unit cell, Z = 4), and comprises a bilayer network of distorted edge-sharing MoO_6 octahedra [14], bonded to adjacent layers by van der Waals forces, and stacked along the [010] crystallographic direction [15]. Small ions are prone to accommodate themselves in the van der Waals gap creating oxygen-deficient α−MoO_3 [16]. Being hydrogen the smallest of elements, it is totally fit to be inserted into the van der Waals gap [17]. While MoO_3 has been broadly adopted as an answer to the electrochemical energy storage dilemma [18–21], these hydrogen-ion storage solutions proved themselves to fulfil a limited function in the renewable energy quest [22]. Solid-state hydrogen storage seems to be a more viable tool, in spite this field being quite new when contrasted with batteries or catalysis studies [23]. Literature reports about α−MoO_3 hydrogenation are indeed quite limited. α−MoO_3 has been hydrogenated as loosen powders [24], single crystal

[25], or thermally evaporated polycrystalline films [26]. Hydrogenation is usually assessed by flowing (pure or diluted in N_2, forming gas) H_2 gas in heated furnaces [25,26], or achieved by plasma reactions in a plasma enhanced chemical vapour deposition system at 180 °C [24]. While hydrogen plasma has been employed, this has been done to make α−MoO_{3-x} nano-powders to be applied as cathode material to lithium ion batteries [27]. In this work, to fill a literature gap, hydrogen plasma was used at room temperature to hydrogenise monocrystalline α−MoO_3 thin films oriented along the [010] direction. Films were deposited *via* atomic layer deposition (ALD) [28,29], an extremely versatile technique [30], compared to (yet adaptable to functionalise) powdered materials [31]. Results showed that the pressure in the chamber played a significant role in the amount of hydrogen incorporated into the layered α−MoO_3 crystal structure, making this a material with great promise for energy storage purposes.

2. Experimental

2.1 Film growth and hydrogen plasma treatment

α−MoO_3 thin films were deposited over *p*−Si (100) substrates by means of ALD, following a growing procedure that we developed earlier [28]. The substrate temperature was set at 400 °C, so as to have [010] oriented α−MoO_3 films with around 40 nm in thickness. Hydrogen plasma treatment was performed in a parallel-plate reactive ion etching reactor (IONVAC, IT). It uses a 13.56 MHz radio frequency signal to generate hydrogen plasma. Specimens were subjected to hydrogen plasma cycles of 18 min varying the pressure in the chamber (500, and 1000 mTorr), and keeping the applied power constant at 80 W. As the parallel plates have the same diameter, 20 cm, the applied power density is relatively low, around 0.25 $W.cm^{-2}$.

2.2 Characterisation

Immediately after being subjected to plasma treatment, α−MoO_3 films were analysed by means of X-ray diffraction (XRD) techniques. Grazing incidence XRD (GIXRD) was used to detect the mineralogy of plasma treated films. This was done at room temperature on a Malvern PANalytical X'Pert Pro MRD diffractometer equipped with a fast PiXcel detector using CuK_α radiation generated at 40 kV and 40 mA. GIXRD patterns were recorded at an incident angle of 0.5°, with a step size of 0.01 °2θ, a counting time of 0.5 s, over the 5–55 °2θ interval. All of the GIXRD measurements were assessed orienting the films along the (100) reflection of the Si substrate, used as reference peak, to have reliable values of the α−MoO_3 unit cell parameter *b*. The same instrument was used to collect specular X-ray reflectivity (XRR) patterns. This was done to retrieve information about the thickness, root mean square (RMS) surface roughness, and density of the films. XRR measurements were recorded in parallel beam geometry, with incidence angle from 0 to 4 °2θ, a step size of 0.001 °2θ, and a

counting time of 0.5 s. XRR patterns were fitted using the X'Pert Reflectivity software package; the sample model involved a α−MoO_3/native SiO_2/Si stack with surface and interface roughness. Scanning electron microscopy (SEM) micrographs were acquired on a Zeiss Merlin, operating at 5 kV. Raman spectra were collected on a MicroRaman Spectra-C spectrometer (SOLAR TII), equipped with a 632 nm laser as the excitation source, in the 100-1100 cm^{-1} wavenumber range, with 100 s acquisition time.

3. Results and discussion

XRR patterns of the films, before and after the 18 min hydrogen plasma treatment, are shown in Figure 1a; Table 1 lists their thicknesses and RMS surface roughness. Plasma treatment slightly etches the surface of the films, the thickness decreasing of around 3 nm, at both the pressures experienced in the chamber. Likewise, the RMS surface roughness decreases from 2.0 nm to around 1.5 nm at 500, and 1000 mTorr.

Top-view SEM micrographs of untreated α−MoO_3 film (Figure 1c), and that after 18 min hydrogen plasma treatment at 500 mTorr (Figure 1b), show the change in the surface, with the formation of flat areas − as also reported in the inset of Figure 1b. This is in good agreement with the RMS surface roughness decrease estimated by XRR.

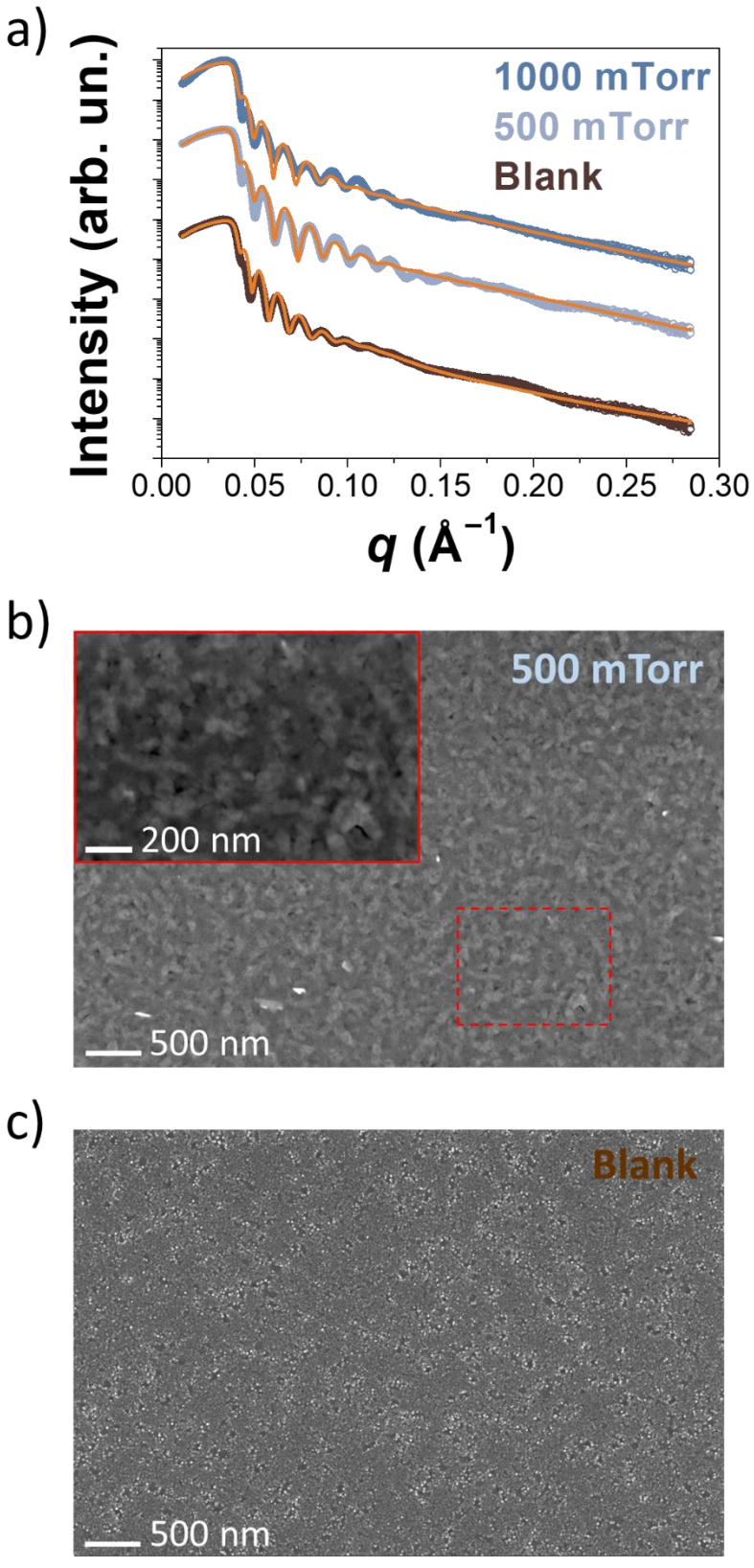

Figure 1 – a) XRR patterns of the specimens before and after hydrogen plasma treatments, log-normal scale. The orange continuous line represents the fittings. SEM micrographs of α−MoO_3 films: b) after 18 min hydrogen plasma treatment, with the pressure in the chamber set at 500 mTorr (the inset reports the film at larger magnification); c) before the plasma treatment.

Table 1 – XRR thickness and RMS surface roughness of the MoO_3 layer as extracted from XRR fittings; unit cell parameter *b* in the analysed samples before and after 18 min hydrogen plasma treatment, as derived from GIXRD.

Sample	Thickness (nm)	RMS (nm)	Unit cell parameter *b* (Å)
Before hydrogen plasma	44.0±0.3	2.0±0.3	13.84
500 mTorr	40.8±0.5	1.5±0.3	14.59
1000 mTorr	41.0±0.5	1.5±0.2	14.35

Figure 2 displays the GIXRD patterns of the α−MoO_3 films before and after the hydrogen plasma treatment at 500 and 1000 mTorr. As we previously detailed in reference [28], the as-deposited MoO_3 film is mostly composed of the orthorhombic α−MoO_3 polymorph. The unit cell parameter *b* of it being 13.84 Å (Table 1), consistent with that of molybdite [32]. From Figure 2, it is clear that, following the hydrogen plasma treatment, disappearance of the β−polymorph and, most importantly, a shift towards lower angles of the (0*k*0) reflections happened (Table 1), this reflecting an expansion in the *b*-axis of molybdite structure.

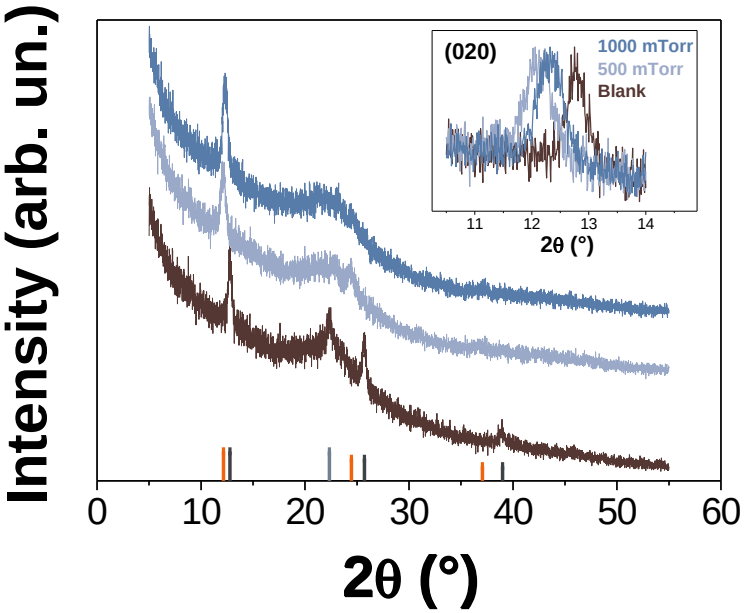

Figure 2 – GIXRD of the specimens before and after hydrogen plasma treatments. The vertical bars represent: the (0*k*0) reflections of α−MoO_3 (dark blue), β−MoO_3 (light blue), and (0*k*0) reflections of hydrogen plasma treated α−MoO_3 at 500 mTorr (orange). The inset reports intensity normalised (020) reflections to highlight the angular shift following the hydrogen plasma treatment.

α−MoO_3 has a layered crystal structure, as shown in Figure 3a,b. Each MoO_6 octahedron has one apical oxygen, in position O1, pointing perpendicular to the van der Waals gap (inset of Figure 3a) [25]. This enables two van der Waals gaps per α−MoO_3 unit cell (yellow planes in Figure 3a,b). The distance between two equivalent O1−O1 – vertically aligned along the [010] − in α−MoO_3 before the plasma treatment is 7.12 Å; that after 18 min hydrogen plasma at 500 mTorr is 7.49 Å. This is therefore pointing out to an expansion in the van der Waals gap of around 0.37 Å. That is greater than the 0.1 Å communicated for oxygen deficient α−MoO_3 nano-belts [33].

[As a comparison, 6 min of hydrogen plasma treatment at 500 mTorr, led to a smaller expansion in the van der Waals gap, around 0.27 Å, compared with that obtained with 18 min, as shown in Figure S1a. As reported below, this is related to a lower hydrogen incorporation in the α−MoO_3 structure.] Thus, besides oxygen reduction, an adsorption of hydrogen as H^+ at O1 sites (Figure 3b) is strongly predictable. Indeed, this has been reported theoretically − by means of density functional theory (DFT) calculations− and experimentally, in previous literature [33–35]. However, the hydrogen surface coverage of α-MoO_3 still remains a topic of debate. While some DFT studies indicate that hydrogen tends to adsorb onto the O1 sites, and then diffuse into the adjacent O1, O2, and O3 sites [36], other state that at low coverage (*i.e.* a single H atom) hydrogen atoms have a tendency to occupy O2 sites over others, while at high coverage (*i.e*. two hydrogen atoms) they tend to preferentially reside on O1 sites [37]. Besides, the reversibility of the process (*vide infra*) provides an indirect indication that no structural change occurred, and that hydrogen is adsorbed in the van der Waals gap, thus at O1 sites [33,38].

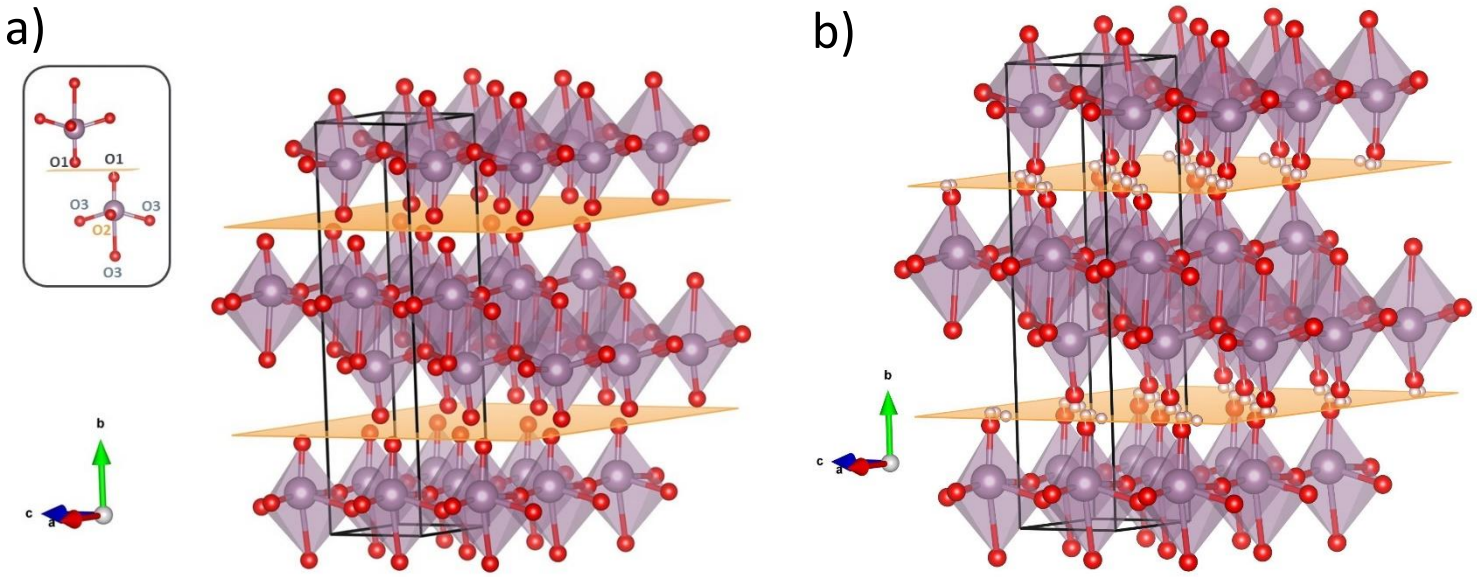

Figure 3 – 3D visualisations of α−MoO_3 drawn with VESTA software suite [39]. Unit cell parameters *b* are from Table 1; unit cell parameters *a* and *c* were taken from reference [32], and kept as constraints in the 3D visualisations. Red spheres are oxygen atoms, violet spheres Mo atoms, small white spheres H atoms. Yellow horizontal planes represent the two van der Waals gaps per α−MoO_3 unit-cell along the [010] direction. The unit cell is defined by the continuous black line. a) Before the plasma treatment; b) after 18 min 500 mTorr plasma treatment. The inset in a) shows the oxygen sites in the MoO_6 octahedra.

By analogy with Li-ion intercalation experiments [27,40], being the expansion in the unit cell parameter *b* higher in the specimen treated with hydrogen plasma with the chamber at 500 mTorr than in that at 1000 mTorr (Table 1), it follows that the former set-up is more effective in storing hydrogen in α−MoO_3. Indeed, by using a chamber pressure of 500 mTorr, the measured DC_{bias} during the plasma treatment, at the radio frequency power of 80 W, was about 205 V. Conversely, with the pressure in the chamber at 1000 mTorr, this was lower, being ~135 V. As already demonstrated for conventional implantation processes [41,42], a higher bias allows for a more efficient ion injection into the films. Hence, the process at 500 mTorr leads hydrogen to be more effectively injected in α−MoO_3.

Considering the *b*-expansion in the α−MoO_3 unit cell of the specimen treated with the chamber at 500 mTorr, assuming that two H atoms accommodated themselves at each O1 as proposed in reference [37] (*i.e.* 8 H atoms per unit cell), and a 1 cm^2 α−MoO_3 film with 40 nm in thickness, we can roughly estimate a hydrogen storage of 2.5×10^{-7} moles. From XRR we know that the density of the α−MoO_3 is 4.0 $g.cm^{-3}$, therefore, the ratio between the molar mass of adsorbed hydrogen and that of α-MoO_3 is about 1.55 wt%. This is in line with what reported in recent literature on a metal hydride system [43].

Raman spectra are displayed in Figure 4. Most of the Raman bands visible in Figure 4 are assigned to the Si substrate. The only detectable Raman bands belonging to α−MoO_3 are those at around 665 and 820 cm^{-1}, assigned to B_{2g}, B_{3g} (O–M–O stretch), and to the A_g Raman modes [44], respectively. The latter band is associated with M=O stretching vibrations along the *b*-axis. A broadening of that band reveals a loss of oxygen [44], as is the case of the specimens that underwent hydrogen plasma treatment. Creating oxygen vacancies allows for the incorporation of hydrogen in the α−MoO_3 structure [25].

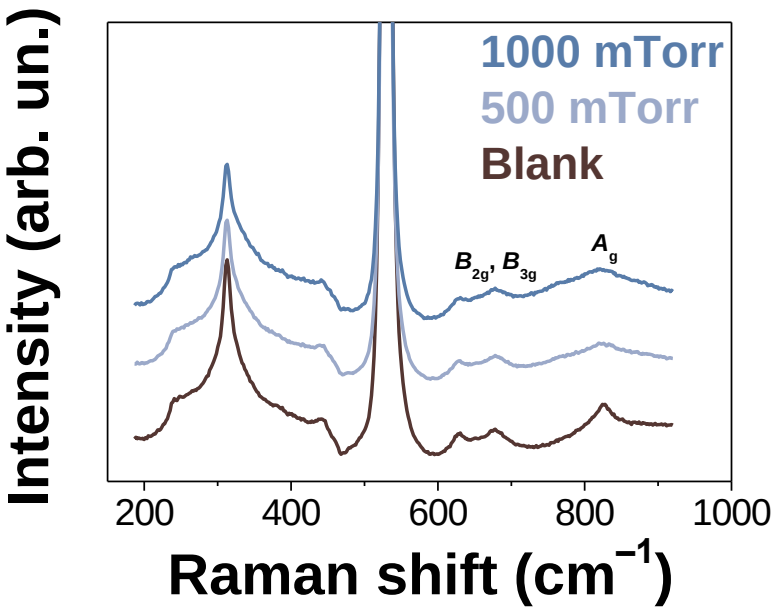

Figure 4 – Raman spectra of specimens before and after hydrogen plasma treatments. α−MoO_3 Raman bands at around 665 and 820 cm^{-1} are shown by their modes (B_{2g}, B_{3g}, and A_g, respectively).

3.1 Reversibility of hydrogenation

To examine the reversibility of the process, the specimen that was treated with hydrogen plasma at 500 mTorr has been stored in air at room temperature (up to 96 h). After that, it was again subjected to hydrogen plasma. GIXRD were recorded again to calculate the % in the expansion, and the following recovering, of the unit cell parameter *b*. As shown in Figure 5, the unit cell parameter *b* expands, and totally recovers itself to the starting value after repeated 18 min hydrogen plasma / 96 h storage in air cycles. This confirms that the layered orthorhombic structure of the parent α−MoO_3 is retained after the hydrogen plasma treatment, and that the process is reversible, unlike what has been described to happen during the initial lithiation of a pristine α−MoO_3 electrode [40]. Through exposure to air, hydrogen adsorbed (at O1 sites) might react with ambient oxygen, leading to the formation of desorbed water [26], thus restoring the original length of α−MoO_3 unit cell parameter *b*. It is worth noting that after the third plasma / recovery in air cycle at 500 mTorr (*i.e.* the last point in Figure 5), the XRR thickness of the film was 40.2±0.2 nm, this showing the coming to a saturation in the surface etching.

To prove the reaction of hydrogen adsorbed at O1 sites with ambient air, specimen after 18 min hydrogen plasma at 500 mTorr was exposed to 24 h N_2 flux directly after the plasma treatment (Figure S1b). As shown in Table S1, virtually no shift in the (0*k*0) reflections happened: we can fairly hypothesise that after N_2 flux hydrogen stayed stored in the α−MoO_3 layered structure. The potential for storing hydrogen on α-MoO_3, and exploring methods for desorbing it at temperatures other than room temperature is currently under investigation.

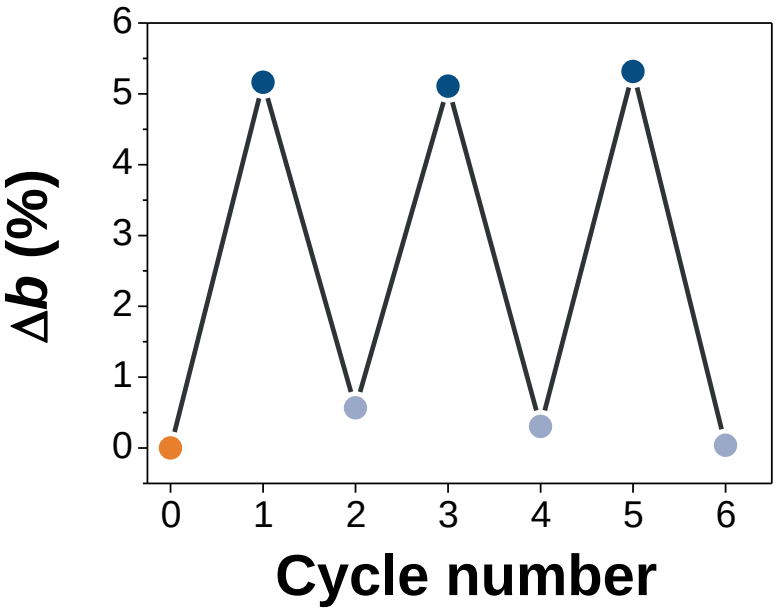

Figure 5 – Percentage in the expansion of the unit cell parameter *b*, depicting the H_2 storage / recovery switches with repeated 18 min plasma at 500 mTorr cycles (dark blue circles) / 96 h exposure in air (light blue circles) cycles. The orange circle represents the untreated specimen.

Conclusions

Hydrogen has the potential to play a significant role in the transition to a more sustainable and decarbonised energy system. However, its actual storage systems are of high cost, low energy density, and undergo safety concerns. While materials-based storage methods display interesting alternatives, a strong candidate for storing hydrogen still lacks. In this work, we have proposed [010] oriented α−MoO_3 thin films as a promising alternative material for solid-state hydrogen storage. It has been shown that hydrogen plasma is a suitable way to hydrogenise, at room temperature and at relatively low pressure, α−MoO_3 thin films. By means of XRD analyses, we have found that hydrogen located itself in the van der Waals gaps along the [010] crystallographic direction. The process has been found to be totally reversible in air, and recoverable after repeated cycles.

Ongoing studies are being conducted to address the handling over the desorption process as a future research direction.

Acknowledgements

The work was supported by the National project “Nano Foundries and Fine Analysis - Digital Infrastructure” (NFFA-DI) - Code: IR0000015, CUP: B53C22004310006 co-financed by the Next Generation EU, the “Tecnopolo per la medicina di precisione” (TecnoMed Puglia) – Regione Puglia: DGR no. 2117 del 21/11/2018 CUP: B84I18000540002 and the project “Hybrid 3D Chiral Metamaterial/2D MoS_2 Phototransistors for Circularly Polarized Light Detection” (HYSPID), CUP: B86C18000430006, funded by the Italian National Research Council. We are very much obliged to Ms Iolena Tarantini (University of Salento) and Mr Gianmichele Epifani (CNR NANOTEC) for technical support. Dr Francesco Gabellone (CNR NANOTEC) is kindly acknowledged for his help in the graphical editing.

Data availability statement

The raw/processed data required to reproduce these findings cannot be shared at this time as the data also forms part of an ongoing study.

References

[1] N. Armaroli, V. Balzani, The Legacy of Fossil Fuels, Chem. – Asian J. 6 (2011) 768–784. https://doi.org/10.1002/asia.201000797.

[2] L. Chen, G. Msigwa, M. Yang, A.I. Osman, S. Fawzy, D.W. Rooney, P.-S. Yap, Strategies to achieve a carbon neutral society: a review, Environ. Chem. Lett. 20 (2022) 2277–2310. https://doi.org/10.1007/s10311-022-01435-8.

[3] United Nations, Net Zero Coalition, U. N. https://www.un.org/en/climatechange/net-zero-coalition.

[4] D.M. Tobaldi, K. Kočí, M. Edelmannová, L. Lajaunie, B. Figueiredo, J.J. Calvino, M.P. Seabra, J.A. Labrincha, Cu_xO and carbon–modified TiO_2–based hybrid materials for photocatalytically assisted H_2 generation, Mater. Today Energy. 19 (2021) 100607. https://doi.org/10.1016/j.mtener.2020.100607.

[5] H. Blanco, A. Faaij, A review at the role of storage in energy systems with a focus on Power to Gas and long-term storage, Renew. Sustain. Energy Rev. 81 (2018) 1049–1086. https://doi.org/10.1016/j.rser.2017.07.062.

[6] F. Dawood, M. Anda, G.M. Shafiullah, Hydrogen production for energy: An overview, Int. J. Hydrog. Energy. 45 (2020) 3847–3869. https://doi.org/10.1016/j.ijhydene.2019.12.059.

[7] A. Kumar, P. Muthukumar, P. Sharma, E.A. Kumar, Absorption based solid state hydrogen storage system: A review, Sustain. Energy Technol. Assess. 52 (2022) 102204. https://doi.org/10.1016/j.seta.2022.102204.

[8] H. Li, X. Cao, Y. Liu, Y. Shao, Z. Nan, L. Teng, W. Peng, J. Bian, Safety of hydrogen storage and transportation: An overview on mechanisms, techniques, and challenges, Energy Rep. 8 (2022) 6258–6269. https://doi.org/10.1016/j.egyr.2022.04.067.

[9] K.L. Lim, H. Kazemian, Z. Yaakob, W.R.W. Daud, Solid-state Materials and Methods for Hydrogen Storage: A Critical Review, Chem. Eng. Technol. 33 (2010) 213–226. https://doi.org/10.1002/ceat.200900376.

[10] M. Osada, T. Sasaki, Two-Dimensional Dielectric Nanosheets: Novel Nanoelectronics From Nanocrystal Building Blocks, Adv. Mater. 24 (2012) 210–228. https://doi.org/10.1002/adma.201103241.

[11] D. Hanlon, C. Backes, T.M. Higgins, M. Hughes, A. O'Neill, P. King, N. McEvoy, G.S. Duesberg, B. Mendoza Sanchez, H. Pettersson, V. Nicolosi, J.N. Coleman, Production of Molybdenum Trioxide Nanosheets by Liquid Exfoliation and Their Application in High-Performance Supercapacitors, Chem. Mater. 26 (2014) 1751–1763. https://doi.org/10.1021/cm500271u.

[12] R.B. Goncalves, R.Q. Snurr, J.T. Hupp, Computational Investigation of Metal Oxides as Candidate Hydrogen Storage Materials, J. Phys. Chem. C. 126 (2022) 18661–18669. https://doi.org/10.1021/acs.jpcc.2c04556.

[13] P.F. Carcia, E.M. McCarron, Synthesis and properties of thin film polymorphs of molybdenum trioxide, Thin Solid Films. 155 (1987) 53–63. https://doi.org/10.1016/0040-6090(87)90452-4.

[14] P.G. Dickens, S. Crouch-Baker, M.T. Weller, Hydrogen insertion in oxides, Solid State Ion. 18–19 (1986) 89–97. https://doi.org/10.1016/0167-2738(86)90092-5.

[15] I.A. de Castro, R.S. Datta, J.Z. Ou, A. Castellanos-Gomez, S. Sriram, T. Daeneke, K. Kalantar-zadeh, Molybdenum Oxides – From Fundamentals to Functionality, Adv. Mater. 29 (2017) 1701619. https://doi.org/10.1002/adma.201701619.

[16] M. Greenblatt, Molybdenum oxide bronzes with quasi-low-dimensional properties, Chem. Rev. 88 (1988) 31–53. https://doi.org/10.1021/cr00083a002.

[17] H. Ge, Y. Kuwahara, H. Yamashita, Development of defective molybdenum oxides for photocatalysis, thermal catalysis, and photothermal catalysis, Chem. Commun. 58 (2022) 8466–8479. https://doi.org/10.1039/D2CC02658A.

[18] X. Wang, Y. Xie, K. Tang, C. Wang, C. Yan, Redox Chemistry of Molybdenum Trioxide for Ultrafast Hydrogen-Ion Storage, Angew. Chem. Int. Ed. 57 (2018) 11569–11573. https://doi.org/10.1002/anie.201803664.

[19] Z. Su, W. Ren, H. Guo, X. Peng, X. Chen, C. Zhao, Ultrahigh Areal Capacity Hydrogen-Ion Batteries with MoO_3 Loading Over 90 $mg.cm^{-2}$, Adv. Funct. Mater. 30 (2020) 2005477. https://doi.org/10.1002/adfm.202005477.

[20] H. Guo, D. Goonetilleke, N. Sharma, W. Ren, Z. Su, A. Rawal, C. Zhao, Two-Phase Electrochemical Proton Transport and Storage in α-MoO_3 for Proton Batteries, Cell Rep. Phys. Sci. 1 (2020) 100225. https://doi.org/10.1016/j.xcrp.2020.100225.

[21] C. Huang, W. Zhang, W. Zheng, The debut and spreading the landscape for excellent vacancies-promoted electrochemical energy storage of nano-architected molybdenum oxides, Mater. Today Energy. 30 (2022) 101154. https://doi.org/10.1016/j.mtener.2022.101154.
[22] F. Xing, Z. Bi, F. Su, F. Liu, Z. Wu, Unraveling the Design Principles of Battery-Supercapacitor Hybrid Devices: From Fundamental Mechanisms to Microstructure Engineering and Challenging Perspectives, Adv. Energy Mater. 12 (2022) 2200594. https://doi.org/10.1002/aenm.202200594.
[23] M. Saad Salman, N. Rambhujun, C. Pratthana, Q. Lai, P. Sapkota, K.-F. Aguey-Zinsou, Chapter 12 - Solid-state hydrogen storage as a future renewable energy technology, in: S. Devasahayam, C.M. Hussain (Eds.), Nano Tools Devices Enhanc. Renew. Energy, Elsevier, 2021: pp. 263–287. https://doi.org/10.1016/B978-0-12-821709-2.00020-7.
[24] J. Zhang, J. Fu, F. Shi, Y. Peng, M. Si, L. Cavallo, Z. Cao, Hydrogen atom induced magnetic behaviors in two-dimensional materials: insight on origination in the model of α-MoO_3, Nanoscale. 10 (2018) 14100–14106. https://doi.org/10.1039/C8NR02670J.
[25] W. Xie, M. Su, Z. Zheng, Y. Wang, L. Gong, F. Xie, W. Zhang, Z. Luo, J. Luo, P. Liu, N. Xu, S. Deng, H. Chen, J. Chen, Nanoscale Insights into the Hydrogenation Process of Layered α−MoO_3, ACS Nano. 10 (2016) 1662–1670. https://doi.org/10.1021/acsnano.5b07420.
[26] J.Z. Ou, J.L. Campbell, D. Yao, W. Wlodarski, K. Kalantar-zadeh, In Situ Raman Spectroscopy of H_2 Gas Interaction with Layered MoO_3, J. Phys. Chem. C. 115 (2011) 10757–10763. https://doi.org/10.1021/jp202123a.
[27] G. Zhang, T. Xiong, M. Yan, L. He, X. Liao, C. He, C. Yin, H. Zhang, L. Mai, α-MoO_{3-x} by plasma etching with improved capacity and stabilized structure for lithium storage, Nano Energy. 49 (2018) 555–563. https://doi.org/10.1016/j.nanoen.2018.04.075.
[28] D. Lorenzo, D.M. Tobaldi, V. Tasco, M. Esposito, A. Passaseo, M. Cuscunà, Molybdenum precursor delivery approaches in atomic layer deposition of α−MoO_3, Dalton Trans. 52 (2023) 902–908. https://doi.org/10.1039/D2DT03702E.
[29] D. Lorenzo, F. Riminucci, M. Manoccio, G. Balestra, D. Simeone, D.M. Tobaldi, M. Esposito, A. Passaseo, V. Tasco, M. Cuscunà, Molybdenum Oxide Functional Passivation of Aluminum Dimers for Enhancing Optical-Field and Environmental Stability, Photonics. 9 (2022) 523. https://doi.org/10.3390/photonics9080523.
[30] R.W. Johnson, A. Hultqvist, S.F. Bent, A brief review of atomic layer deposition: from fundamentals to applications, Mater. Today. 17 (2014) 236–246. https://doi.org/10.1016/j.mattod.2014.04.026.
[31] Y. Hu, J. Lu, H. Feng, Surface modification and functionalization of powder materials by atomic layer deposition: a review, RSC Adv. 11 (2021) 11918–11942. https://doi.org/10.1039/D1RA00326G.
[32] H. Sitepu, B.H. O'Connor, D. Li, Comparative evaluation of the March and generalized spherical harmonic preferred orientation models using X-ray diffraction data for molybdite and calcite powders, J. Appl. Crystallogr. 38 (2005) 158–167. https://doi.org/10.1107/S0021889804031231.
[33] H.-S. Kim, J.B. Cook, H. Lin, J.S. Ko, S.H. Tolbert, V. Ozolins, B. Dunn, Oxygen vacancies enhance pseudocapacitive charge storage properties of MoO_{3-x}, Nat. Mater. 16 (2017) 454–460. https://doi.org/10.1038/nmat4810.
[34] M. Vasilopoulou, A.M. Douvas, D.G. Georgiadou, L.C. Palilis, S. Kennou, L. Sygellou, A. Soultati, I. Kostis, G. Papadimitropoulos, D. Davazoglou, P. Argitis, The Influence of Hydrogenation and Oxygen Vacancies on Molybdenum Oxides Work Function and Gap States for Application in Organic Optoelectronics, J. Am. Chem. Soc. 134 (2012) 16178–16187. https://doi.org/10.1021/ja3026906.
[35] L. Chen, A.C. Cooper, G.P. Pez, H. Cheng, On the Mechanisms of Hydrogen Spillover in MoO_3, J. Phys. Chem. C. 112 (2008) 1755–1758. https://doi.org/10.1021/jp7119137.
[36] X. Sha, L. Chen, A.C. Cooper, G.P. Pez, H. Cheng, Hydrogen Absorption and Diffusion in Bulk α-MoO_3, J. Phys. Chem. C. 113 (2009) 11399–11407. https://doi.org/10.1021/jp9017212.
[37] Y.-H. Lei, Z.-X. Chen, DFT+U Study of Properties of MoO3 and Hydrogen Adsorption on MoO_3(010), J. Phys. Chem. C. 116 (2012) 25757–25764. https://doi.org/10.1021/jp304122n.
[38] T. Tsumura, Lithium insertion/extraction reaction on crystalline MoO_3, Solid State Ion. 104 (1997) 183–189. https://doi.org/10.1016/S0167-2738(97)00418-9.
[39] K. Momma, F. Izumi, VESTA: a three-dimensional visualization system for electronic and structural analysis, J. Appl. Crystallogr. 41 (2008) 653–658. https://doi.org/10.1107/S0021889808012016.

[40] M. Yu, H. Shao, G. Wang, F. Yang, C. Liang, P. Rozier, C.-Z. Wang, X. Lu, P. Simon, X. Feng, Interlayer gap widened α-phase molybdenum trioxide as high-rate anodes for dual-ion-intercalation energy storage devices, Nat. Commun. 11 (2020) 1348. https://doi.org/10.1038/s41467-020-15216-w.
[41] D. Fink, J. Krauser, D. Nagengast, T.A. Murphy, J. Erxmeier, L. Palmetshofer, D. Bräunig, A. Weidinger, Hydrogen implantation and diffusion in silicon and silicon dioxide, Appl. Phys. A. 61 (1995) 381–388. https://doi.org/10.1007/BF01540112.
[42] E. Rimini, Ion implantation: basics to device fabrication, Kluwer Academic Publishers, Boston, 1995.
[43] J. Li, Y. Guo, X. Jiang, S. Li, X. Li, Hydrogen storage performances, kinetics and microstructure of $Ti_{1.02}Cr_{1.0}Fe_{0.7-x}Mn_{0.3}Al_x$ alloy by Al substituting for Fe, Renew. Energy. 153 (2020) 1140–1154. https://doi.org/10.1016/j.renene.2020.02.035.
[44] M. Dieterle, G. Weinberg, G. Mestl, Raman spectroscopy of molybdenum oxides, Phys. Chem. Chem. Phys. 4 (2002) 812–821. https://doi.org/10.1039/B107012F.

Graphical Abstract